

Image analysis of characteristics of fluctuations of thermal mannequin's surface temperature distributions using time series infrared images

Akinaru IINO*, Tetsuo ANNAKA*, Yukari IINO** and Masaaki OHBA***

(Received Oct. 31, 2008)

The final goal of this study was to propose a visualization method of heat transfer distributions over the human body in the indoor environment under cross ventilation conditions. Distributions of thermal mannequin's surface temperature fluctuations were visualized by image processing on infrared animations recorded at 30Hz sampling rate, and their characteristics were analyzed, as the first step of this study.

At first, the influence of air velocity fluctuations on surface temperature fluctuations of thermal mannequin was visualized in the experimental room under cross ventilated cases and under air conditioned cases. An image processing method to transfer the infrared animations to power spectrum images was proposed in order to clarify the frequency of surface temperature fluctuations. And the distributions of sensible heat on thermal mannequin's surfaces were also visualized by classifying the pixels of power spectrum images by the cluster analysis and calculating the correction coefficient that was defined on each cluster for multiplying to roughly estimated value of sensible heat using the mean heat transfer coefficient.

Keywords: thermal image, thermal mannequin, surface temperature, cross ventilation, image analysis

1. INTRODUCTION

Cross ventilation can be effective from the point of energy consumption and greatly improve occupants' thermal comfort. In order to quantify and to evaluate its effectiveness, some studies have pointed out the great influence of airflow fluctuation on heat balance of human bodies under cross ventilation^{1),2),3)}. But it was thought to be difficult to analyze relationship between airflow fluctuation and heat balance of human bodies because of no way of simultaneous measurement of fluctuations of air velocity, air direction and skin temperatures.

The development of thermal graphical devices with the construction function of rapid infrared animations has been progressed, so time series of the skin temperature distributions of human bodies can be recorded at high sampling rate. Infrared animations can be related to fluctuations of air velocity and air direction around human bodies measured by ultrasonic anemometer using image processing technology.

In this research following two measurement devices were focused on; the infrared thermal camera that could record thermal images at 30Hz sampling rate, and the thermal mannequin that could measure time series of generated heat at each body segment. Basic ideas of image processing method to analyze relationship between airflow fluctuation, surface temperatures and amount of generated heat were presented.

2. EXPERIMENTAL METHODS

A sedentary naked thermal mannequin's surface temperatures and sedentary human subjects' skin temperatures were simultaneously measured by infrared thermal camera in a room of KSI building of Urban Renaissance Agency located in Hachioji, Japan, during clear sky days in August, 2006. Inside walls were covered by insulation boards in order to create uniform radiant environment

1) Department of Architecture and Building Engineering, Professor, Dr.Eng.

2) Takahashi Industry Contents, M.Eng.

3) Niigata Seiryō University, Lecturer, Dr.Eng.

4) Tokyo Polytechnic University, Professor, Dr.Eng.

in all experimental cases. The infrared images could be recorded by the infrared thermal camera at 30Hz sampling rate. Air velocity was instantaneously measured by ultrasonic anemometers at 20Hz sampling rate. Air temperatures were simultaneously measured by thermocouples at 1 minute sampling rate. The period of each experimental case was 20 minutes.

Fig.1 expresses the plan of the experimental room and Table 1 shows the outline of the experiment. The thermal mannequin (clo value was 0) and the human subjects (clo value was 0.05) were seated on the chairs at shaded areas in the room. North-side and south-side windows of the room were opened in cross ventilated cases, and the direction of cross ventilation was almost south during the experimental period. All windows were closed in air conditioned cases.

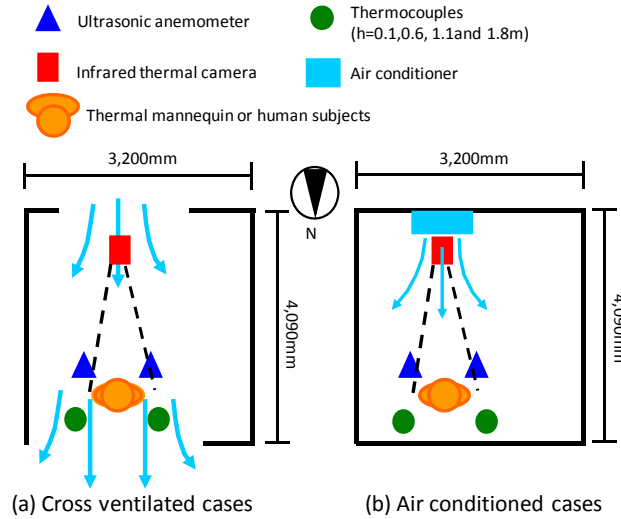


Fig.1 Plan of experimental room

Table 1 Outline of experiment

Case	CV-TM	AC-TM	CV-S1	AC-S1
Time	9:00-9:20	16:32-16:52	17:10-17:30	17:38-17:58
Wind condition	Cross ventilated	Air conditioned	Cross ventilated	Air conditioned
Subject	Thermal mannequin		Human subject	
Mean room temp [°C]	29.2	28.0	29.2	27.7
Mean humidity [%]	73	58	70	56
Mean air velocity [m/s]	0.59	0.81	0.88	0.76

3. BASIC IDEAS OF IMAGE ANALYSIS

Visualization regarding influence of airflow fluctuations on surface temperature distributions of thermal mannequin

Air velocity data were normalized by the exponential function as shown in equation (1), and were compared to surface temperature data of the thermal mannequin.

$$f(\beta, t) = e^{-\beta(68.2-t)} \quad (0 \leq \beta < 1) \quad (1)$$

where

f = weight function,

β = parameter that is variable from 0 to 1, and

t = time [second(s)].

Then correlation coefficients between normalized air velocity and surface temperatures could be calculated for each pixel on infrared images. Its distribution could be visualized by the image

analysis as shown in Fig.2 [Image Processing A]. To calculate correlation coefficients between air velocity and surface temperatures of the thermal mannequin, some items were devised as follows; 1) Infrared thermal camera and ultrasonic anemometer could not start to measure at the exact same time in each case, so each data were translated to frequency space by Fourier transform for time direction. The correlation coefficients were calculated using power spectrum profiles of both the data. And 2) the sampling rate of air velocity was 20Hz and that of surface temperatures was 30Hz, so both data of every 0.1 second could be correlated.

However, air velocity was measured only in front of the thermal mannequin's chest, so the images of correlation coefficients might show the small values on far segments from the chest.

Visualization of power spectrum distributions of thermal mannequin's surface temperature fluctuations

8192 images (=4 minutes and 33 seconds images) were extracted from infrared animations in each experimental case, and Fast Fourier Transform was performed for time direction in each pixel. The Fig.2 [Image Processing B] illustrated the flow of image processing. 4096 monochrome power spectrum images could be constructed. Because of sampling rate was 30Hz, power spectrum images of 5-6 Hz or less frequency might have the effective physical meanings from the point of influence of fluctuation of air velocity.

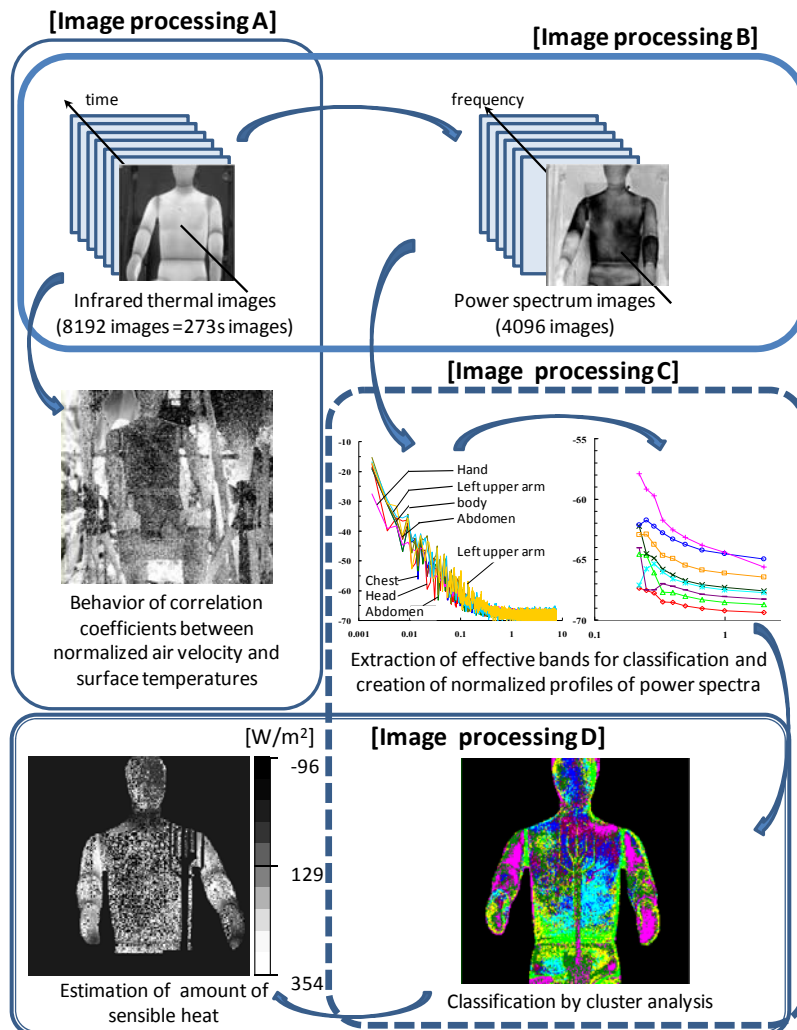


Fig.2 Flow of image processing

Visualization regarding distributions of sensible heat on thermal mannequin's surface

Assuming that turbulence of cross ventilation greatly influenced on instant change of the thermal mannequin's surface temperatures, some power spectrum images were extracted from the point of frequency ranges that represented fluctuations of cross ventilation. Each pixel could be classified by cluster analysis as shown in Fig.2 [Image processing C].

And each cluster was considered to have a unique value of Γ which was defined by following equation (2)-(4);

$$Q_{x_measured} = Q_{x_estimated} + \Delta Q_x \quad (2)$$

$$Q_{x_estimated} = \alpha_t(T_{sx} - T_{ax}) \quad (3)$$

$$\Delta Q_x = \sum_{\text{cluster } y \text{ (on body segment } x)}^N (A_{xy} * \Gamma_y) \quad (4)$$

where

Q_x = amount of sensible heat from body segment 'x' [W/m²]

α_t = total heat transfer coefficient calculated with mean air velocity [W/m²K],

T_{sx} = mean surface temperature of body segment 'x' [K],

T_{ax} = mean air temperature near body segment 'x' [K],

ΔQ_x = difference between measured and estimated sensible heat amounts at body segment 'x' [W/m²],

A = area of each cluster on body segment [m²],

Γ_y = correction coefficient at cluster 'y', and

N = number of clusters.

The correction coefficient Γ should be multiplied to its area and the results should be accumulated in each body segment, and also be added to roughly estimated amount of sensible heat $Q_{x_estimated}$ which had been calculated using heat transfer coefficient estimated with mean air velocity in each case. Γ values could be solved by simultaneous equations (5), because the number of Γ s was equal to the number of body segments of which generated heat amount had been already measured, as shown in Fig.2 [Image processing D] .

$$\begin{pmatrix} A_{11} & A_{12} & A_{13} & \dots & A_{1N} \\ A_{21} & A_{22} & & \dots & \\ A_{31} & & & \ddots & \\ & \vdots & & \ddots & \\ A_{N1} & A_{N2} & A_{N3} & \dots & A_{NN} \end{pmatrix} \begin{pmatrix} \Gamma_1 \\ \Gamma_2 \\ \vdots \\ \Gamma_N \end{pmatrix} = \begin{pmatrix} Q_{1_measured} - Q_{1_estimated} \\ Q_{2_measured} - Q_{2_estimated} \\ \vdots \\ Q_{n_measured} - Q_{n_estimated} \end{pmatrix} \quad (5)$$

where

A_{xy} = number of pixels of cluster 'y' on body segment 'x' (known),

$Q_{x_measured} - Q_{x_estimated}$ = difference between measured and estimated sensible heat amount at body segment 'x' that might be related in turbulence intensity [W/m²] (known).

4. RESULTS AND CONSIDERATIONS

Data of thermal mannequin's surface temperatures were extracted from recorded infrared

images. Fig.3 shows the correspondence of normalized air velocity and surface temperatures at mannequin's chest or at right upper arm. The range of air velocity was 0.8-1.7 [m/s, at $\beta=1.0$] and the range of surface temperature was 32.65-32.70 [°C] at chest and 33.60-33.75 [°C] at right upper arm. It's clear that the fluctuation of air velocity influenced on surface temperatures. And the value of β which brought a good correspondence seemed to differ at each body segment of the mannequin.

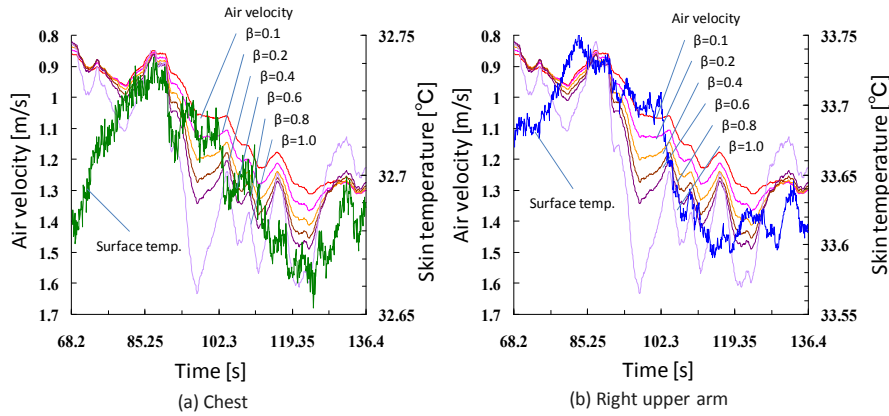


Fig. 3 Examples of relationship between normalized air velocity and surface temperatures of thermal mannequin under the cross ventilated case

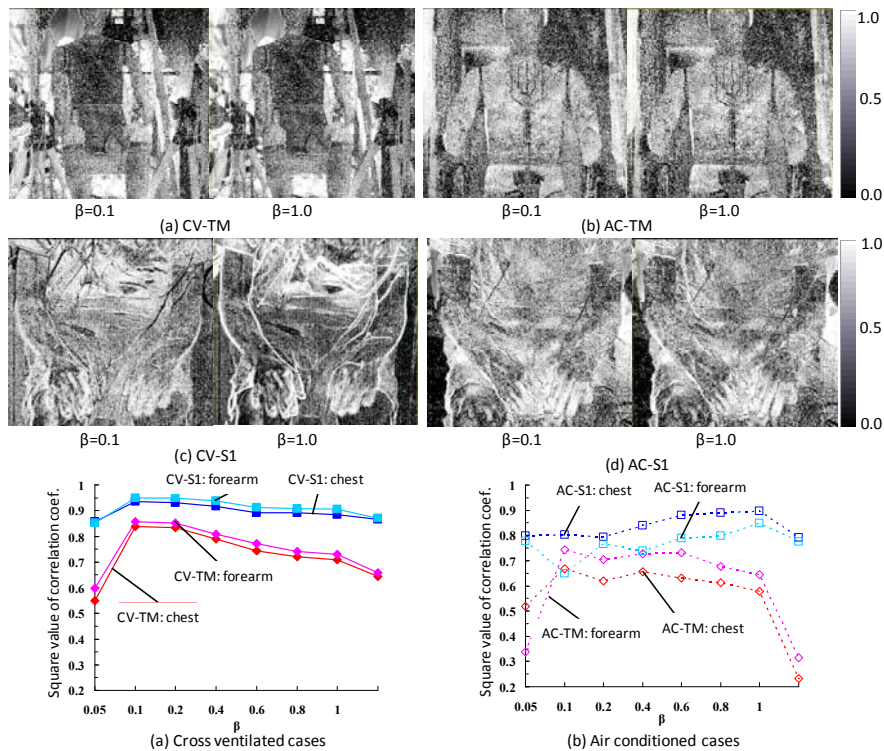


Fig.4 Distribution of correlation coefficients between surface temperature and normalized air velocity

The correlation coefficients between the two for each pixel could be visualized by constructing monochrome images as shown in Fig.4. Correlation coefficients showed 0.58-0.88 in cross ventilated cases and 0.23-0.90 in air conditioned cases. And correlation coefficients at the forearms showed almost larger values than those at the chest.

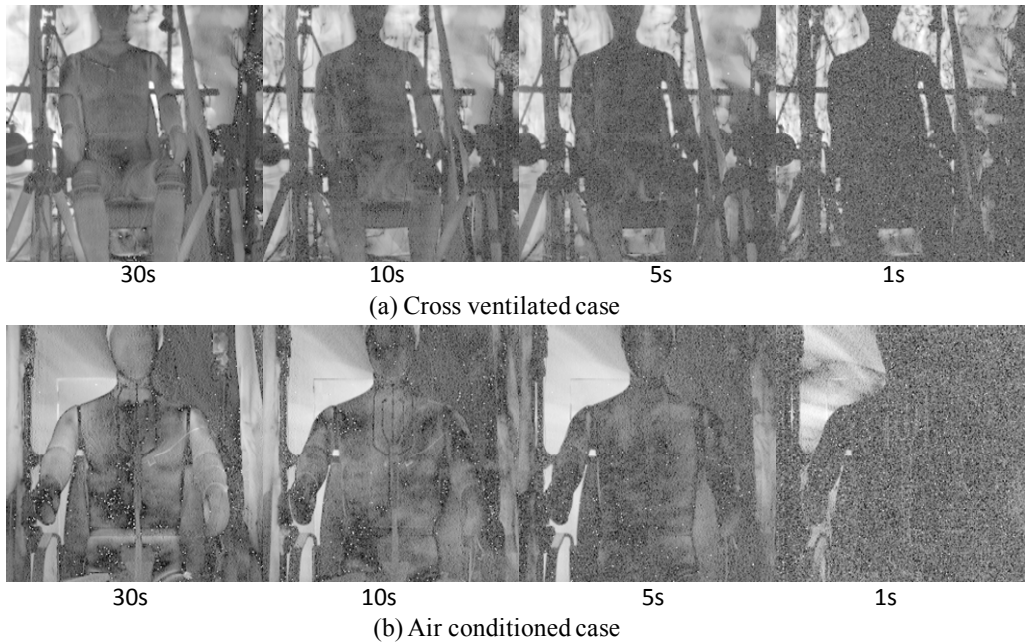


Fig.5 Examples of power spectrum images of thermal mannequin

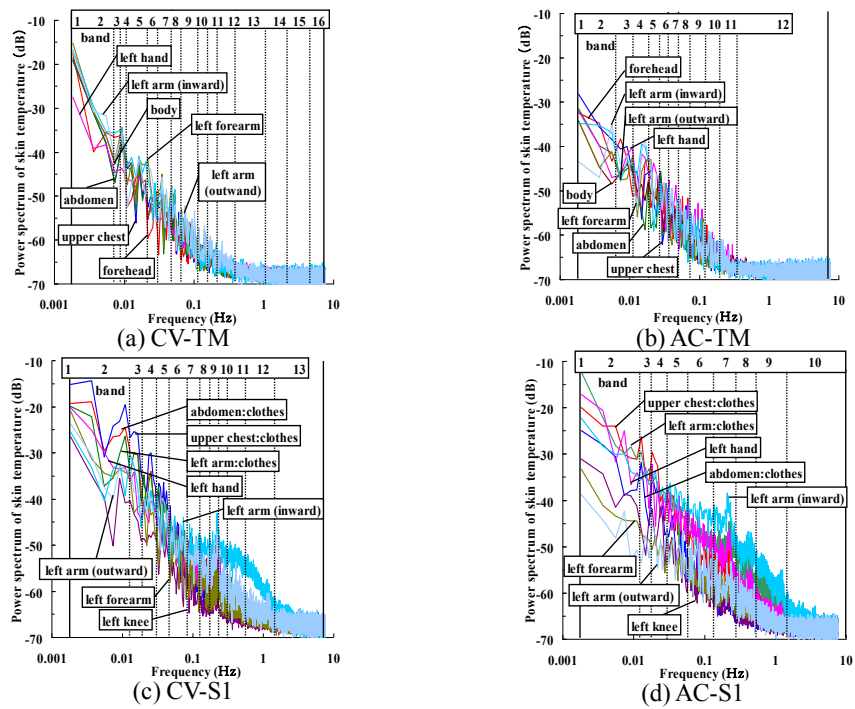


Fig.6 Power spectra of surface temperatures of body segments

Fig.5 shows the examples of power spectrum images. In air conditioned case of the thermal mannequin, power spectra of chest and upper arms showed larger values at 30 seconds (0.03Hz), but smaller values at 10 seconds (0.1Hz). Only sand storm patterns were expressed in images of high frequency at 10Hz or more. In all cases upper arms showed large power spectra at 0.01-0.05Hz, as shown in Fig.6.

The power spectrum images were considered to express the influence of airflow fluctuations. The cluster analysis was performed to power spectrum images. The differences of the power spectrum patterns were visualized as shown in Fig.7. The areas of respective cluster group of the thermal mannequin and the human subjects in air conditioned cases showed larger values than those in cross ventilated cases, because of various wind directions in cross ventilated cases.

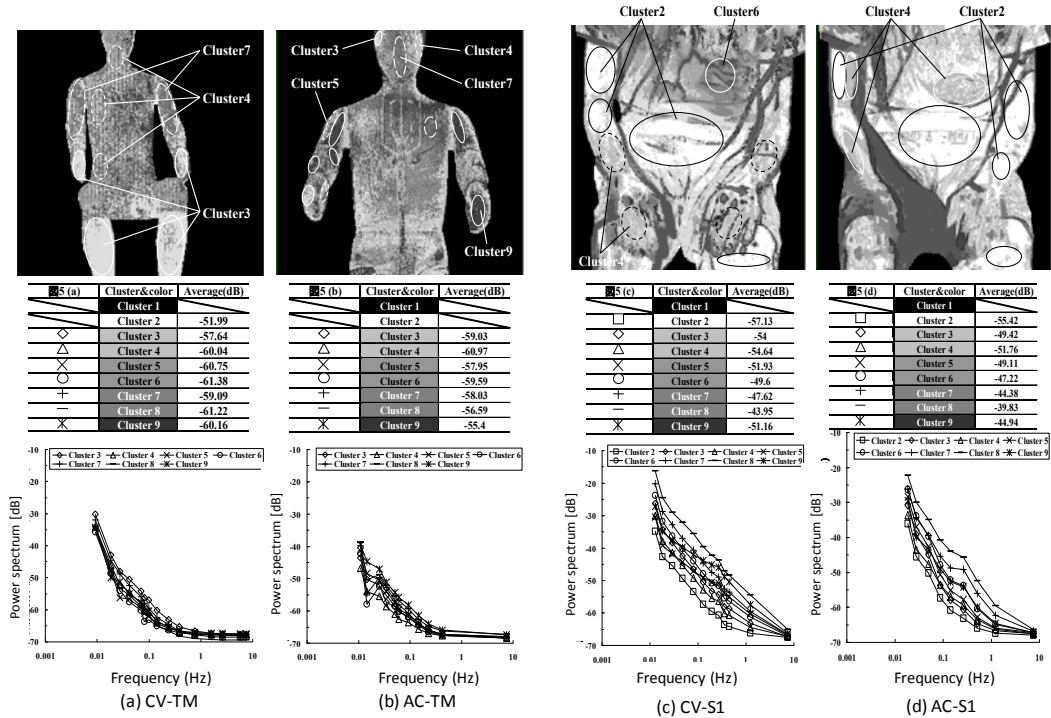


Fig. 7 Results of cluster analysis

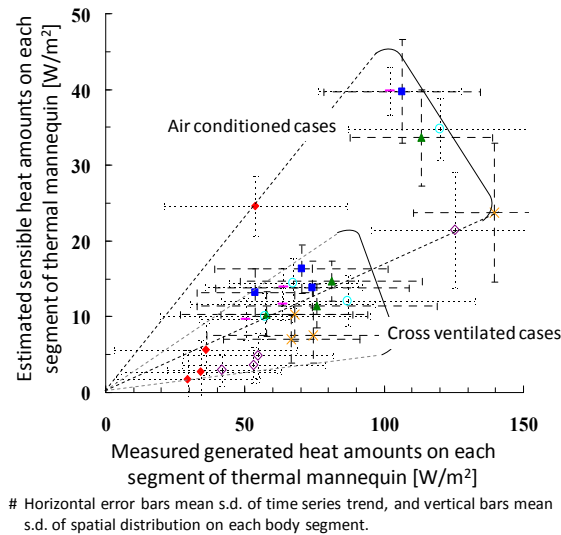


Fig. 8 Comparison of measured and estimated heat amounts

Fig.8 illustrated the sensible heat in each body segment of the thermal mannequin that was roughly calculated using heat transfer coefficient which was estimated with mean air velocity in 28 cases. Estimated heat amounts showed 20-50% of measured heat amounts at each body segment of the mannequin. One reason might be indicated that estimated difference between surface temperatures and air temperatures were small. Another reason could be pointed out that estimated

heat transfer coefficients were small because mean air velocity was only considered and the turbulence intensity was not considered^{4),5)}. Images of estimated Γ values were constructed as shown in Fig.9. Γ values on chest and abdomen segment were larger than those on other body segments. Fig.10 shows the relationship between the ranges of frequencies and the number of bands. Γ values were larger than expected values, but appropriate values of Γ were obtained in the case of 0.1-2.0Hz and around 10 bands.

The Γ values were influenced by number and frequencies of power spectrum images used for the cluster analysis. The number and the locations of body segments which generate heat might also influence on the estimation results. The proof of the idea of estimating sensible heat amounts using heat flux meters, and the clarification of the effective bands for classification will be important in the next stage of our study.

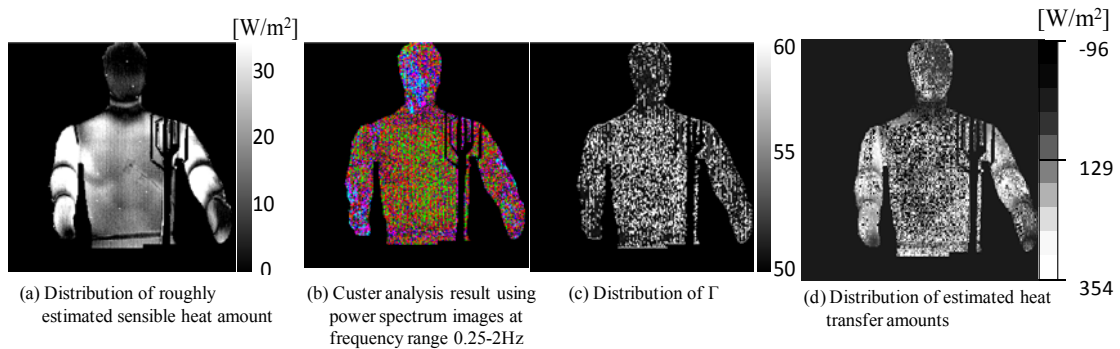


Fig. 9 Examples of image processing results of estimating sensible heat distributions

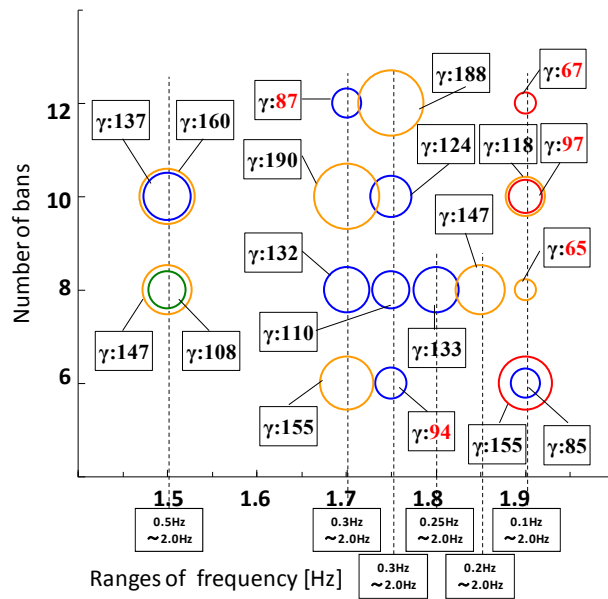


Fig.10 Γ values under 2 variables; ranges of frequency and number of bands

5. CONCLUSIONS

The fluctuations' characteristics of surface temperature of thermal mannequin and human subjects under cross ventilation environment and air conditioned environment were clarified based on the experimental results and the calculation results of FFT and cluster analysis. The effects for analyzing relationship between surface temperature fluctuations and airflow fluctuations were

presented using the infrared animations recorded at 30Hz sampling rate.

The method to construct power spectrum images by Fast Fourier Transform for time direction was proposed. The effective method for estimating amount of sensible heat on thermal mannequin's surfaces was shown by the cluster analysis of the power spectrum images and by the proposition of correction coefficient Γ which could correct amounts of sensible heat on skin surfaces that were roughly estimated using total heat transfer coefficients calculated with mean air velocity.

ACKNOWLEDGEMENTS

This study was supported Wind Engineering Research Center, Tokyo Polytechnic University as part of research program "21st century COE program - Wind Effects on Buildings and Urban Environments." The authors wish to thank Professor Kurabuchi, T., Tokyo University of Science, and Iwamoto, S., Kanawagawa University and Kodera S., Urban Renaissance Agency, for their kind advice and kind arrangement on several measurement devices.

REFERENCES

- 1) Ken Persons (2003), *Human Thermal Environments*, Taylor & Francis, 2nd edn, New York, 31-48.
- 2) *ANSI/ASHRAE Standard 55-2004*, "Thermal Environmental Conditions for Human Occupancy", p.6
- 3) Yukari Iino, Masaaki Ohba, Akinaru Iino and Tetsuo Annaka (2007), "Study on Evaluations of Thermal Environment under Cross Ventilation and Airflows from Air-conditioning System and Electric Fan", *Proc. of IAQVEC Vol.1*, 875-881.
- 4) Tomoko Hirano, Yasuo Kuwasawa and Yuzo Sakamoto (2000), "Effects of Fluctuating Air Movement on Thermal Confort", *Proc. of annual meeting of AIJ*, 413-414 (in Japanese).
- 5) Takeshi Ono, Shuzo Murakami, Ryuzo Ooka and Tsuyoshi Saotome (2005), "Evaluation of Mean Convective Heat Transfer Coefficient of a Human Body in Outdoor Environments", *Proc. of annual meeting of AIJ*, 653-654 (in Japanese).